Macromolecules

Article

Cite This: Macromolecules 2018, 51, 5409−5419

Elastic Constants of Chromonic Liquid Crystals

Emanuele Romani,[†] Alberta Ferrarini,*[,‡] and Cristiano De Michele*[,†]

[†]Dipartimento di Fisica, "Sapienza" Università di Roma, P.le A. Moro 2, 00185 Roma, Italy

[‡]Dipartimento di Scienze Chimiche, Università di Padova, via Marzolo 1, I-35131 Padova, Italy

Supporting Information

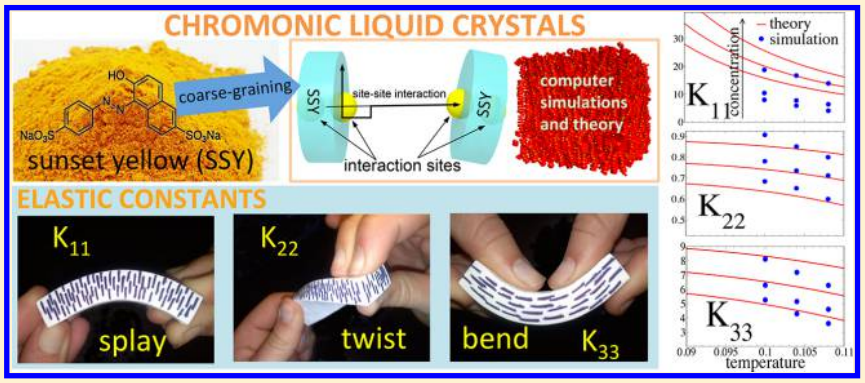

ABSTRACT: Chromonics are a class of liquid crystals made of aqueous solutions of plank-like molecules, which self-assemble into semiflexible chains. At a given temperature a nematic phase is formed when the system reaches a sufficiently high concentration. Among the unusual properties of chromonic liquid crystals, particularly prominent is the large anisotropy of elastic constants, which leads to new phenomenologies in confined volumes. To gain insights into the microscopic origin of this behavior, we have investigated the elastic properties of a model system that undergoes self-assembly driven nematization by using Monte Carlo simulations and an Onsager-like theory. The relative magnitude of the elastic constants and their dependence on temperature and density show the distinguishing features found in chromonic liquid crystals. We identify the relevant microscopic determinants of this behavior, and we discuss the role played by both the molecular self-assembly and the intrinsic flexibility of aggregates.

INTRODUCTION

Chromonics are a class of lyotropic liquid crystals (LCs) formed by aqueous solutions of molecules that have a multiring aromatic core with peripheral hydrophilic groups.[1,2] Typical examples are drugs, nucleic acids, and dyes, such as 6-hydroxy-5-[(4-sulfophenyl)azo]-2-naphthalenesulfonic acid, also known as sunset yellow (SSY), and disodium cromoglycate (DSCG). When dissolved in water, these molecules self-assemble by face-to-face stacking into columnar aggregates, which beyond a certain concentration form a nematic (N) phase, and then a hexagonal columnar phase at even higher concentration. These systems provide a relevant example of the interplay between self-assembly and order.

Chromonic liquid crystals have a number of special features which make them useful for applications. For instance, unlike most liquid crystals, chromonics are biocompatible; they are nontoxic to many microbial species and do not alter antibody−antigen binding. They exhibit also a special elastic behavior, which originates from a large anisotropy of the elastic constants. This yields a variety of unusual phenomena. The low cost for twist deformations leads to spontaneously twisted (chiral) configurations around colloidal particles and under confinement to curved geometries.[3−7] Another impressive effect is that the breadth of defect cores, i.e., regions over which the orientational order parameter changes, reaches tens of micrometers, so allowing direct observation by optical microscopy.[8] Elastic properties and biocompatibility have been exploited in the so-called living liquid crystals, where chromonics are used as a medium for motile bacteria.[9−13] The propulsive forces generated by bacteria, of the order of tens of pN, are comparable in magnitude to elasticity mediated forces, which makes chromonics suitable to explore the behavior of active soft matter.

Detailed experimental investigations of the elastic properties were reported for SSY[14,15] and for DSCG,[16] and it was found that their behavior could not be explained by the existing theories. Liquid crystals oppose a resistance to distortion of the director, i.e., the average alignment axis, and their bulk elasticity is described in terms of three fundamental modes, i.e., splay, twist, and bend,[17] with the corresponding moduli denoted as K_{11} (splay), K_{22} (twist), and K_{33} (bend). The elastic properties of low molar mass thermotropic liquid crystals have been widely investigated, both experimentally and theoretically, and several aspects of their dependence on the molecular

Received: April 28, 2018
Revised: June 11, 2018
Published: July 13, 2018

DOI: 10.1021/acs.macromol.8b00900
Macromolecules 2018, 51, 5409−5419

structure are presently understood (see refs 18 and 19 for a review). The usual relationship is $K_{22} < K_{11} < K_{33}$, although in the past few years an anomalously low bend elastic constant was evidenced in the case of mesogens that have a bent shape, such as liquid crystal dimers[20] and bent-core molecules.[21] Comparatively few measurements of elastic constants have been reported for polymer systems. There is agreement on K_{22} being the smallest of the three elastic constants, but the relative magnitudes of splay and bend constants depend on the particular system. For thermotropic liquid crystal polymers, K_{11} larger than K_{33} by at most an order of magnitude can be found.[22,23] For lyotropic systems, different behaviors are reported, which are generally related to the polymer flexibility. For colloidal suspensions of tobacco mosaic virus (TMV) K_{33}/K_{11} of the order of 10 were reported.[24,25] On the other hand, for solutions of poly(γ-benzylglutamate) (PBG) the dependence of K_{11}/K_{33} on molecular weight was evidenced; in most cases values range from around 0.7 to around 1.2,[26] but also ratios of the order of 1000 were measured.[27]

The elastic constants of polymer liquid crystals are expected to strongly depend on the molecular flexibility. For hard rigid rods (HR), the relevant molecular quantity is the aspect ratio, between the contour length $\mathcal{L}$ and the diameter D. The following expressions were obtained:[28]

$$K_{11}^{HR} = \frac{7}{8\pi}\frac{k_B T}{D}\frac{\mathcal{L}}{D}\Phi$$

$$K_{22}^{HR} = \frac{7}{24\pi}\frac{k_B T}{D}\frac{\mathcal{L}}{D}\Phi$$

$$K_{33}^{HR} = \frac{4}{3\pi^2}\frac{k_B T}{D}\left(\frac{\mathcal{L}}{D}\right)^3\Phi^3 \quad (1)$$

where k_B is the Boltzmann constant, T is temperature and Φ is the volume fraction. The relative trend is the same as for low molar mass liquid crystals, with $K_{11} = 3K_{22}$ and K_{33} that can become much larger than the other two constants with increasing length. Equations 1 were obtained considering the excluded volume cost for distortion of the nematic director. For splay deformations of polymeric systems an additional cost has to be taken into account, which originates from the decrease of entropy caused by the restricted distribution of polymer ends, at constant concentration.[29] The following expression is obtained using the ideal gas approximation:[30]

$$\Delta K_{11} = \frac{4}{\pi}\frac{k_B T}{D}\Phi\frac{\mathcal{L}}{D} \quad (2)$$

For long polymers this contribution becomes very large and is expected to dominate over the energetic cost for splay deformations. Semiflexible (SF) polymers are characterized by another length scale, the persistence length λ_p, and the expressions for the twist and bend elastic constants become[30,31]

$$K_{22}^{SF} = \frac{k_B T}{D}\left(\frac{\lambda_p}{D}\right)^{1/3}\Phi^{1/3} \quad (3)$$

$$K_{33}^{SF} = \frac{4}{\pi}\frac{k_B T}{D}\frac{\lambda_p}{D}\Phi \quad (4)$$

Equation 2 can be used also in the case of semiflexible polymers; actually, for long semiflexible polymers the splay elastic constants is generally identified just with ΔK_{11}.[30,31]

Chromonics not only are flexible but also, as reversible polymers, have the feature of a distribution of lengths, which is affected by temperature and concentration. The rigid rod model is clearly inadequate to describe the behavior of their elastic constants:[14,16] it predicts $K_{11}/K_{22} = 3$, irrespective of temperature and concentration, whereas measured values are much higher and decrease with decreasing concentration and increasing temperature. Likewise, the predicted K_{11}/K_{33} is significantly lower than experimental values and has the wrong dependence on concentration (decreases rather than increasing with increasing Φ). The expressions for semiflexible polymers, eqs 3 and 4 together with eq 2, are more appropriate to account for the behavior of the elastic constants of chromonics. However, using reasonable estimates of Φ and λ_p, values of K_{22}/K_{33} up to an order of magnitude larger than the measured ones are obtained for DSCG[16] and SSY.[14] For long semiflexible polymers, from eqs 3 and 4 one obtains $K_{11}/K_{33} = \mathcal{L}/\lambda_p$; for chromonics this ratio will depend on temperature and concentration, since these may affect the length distribution and the persistence length of aggregates.

Chromonic liquid crystals were investigated by atomistic molecular dynamics simulations,[32,33] which provided insights into the structure of aggregates and the mechanism of aggregation. Theory and Monte Carlo simulations with coarse-grained models were used to describe the phase behavior of systems undergoing linear polymerization as a function of temperature and concentration.[34−38] In a very recent paper, both phase behavior and elastic properties of chromonic liquid crystals were investigated by Monte Carlo simulations, using a Gay−Berne coarse-grained model.[39] In the latter work elastic constants ratios of the order of the unity were found, similar to those of conventional thermotropic liquid crystals. Here, we address the same problem using a different model, similar to that adopted to describe the liquid crystal behavior of self-assembling DNA oligomers.[38,40,41] Chromonic molecules are represented as hard disks of thickness $\mathcal{L}_d$ and diameter D (see Figure 1), decorated with

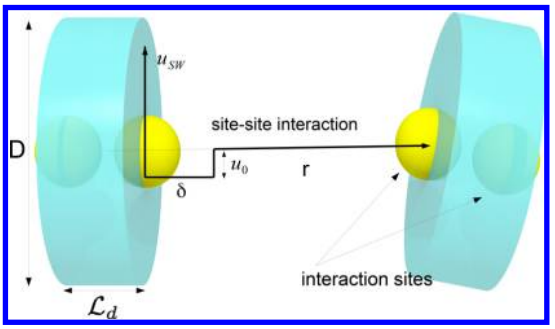

Figure 1. Model used in this work.

two attracting sites. We have taken model parameters appropriate for SSY, which forms a nematic phase whose viscoelastic properties were recently measured.[14] The aggregate structure of aqueous solution of SSY has been rather well characterized:[32,42−44] stacks were found to contain one molecule in cross section and to have an average diameter of about 1 nm[44] or 1.4 nm.[45] In the present study, Monte Carlo simulations are complemented by theory: an Onsager-like approach, which was proposed to evaluate the chiral strength and twist elastic constant of the cholesteric phase of DNA oligomers,[46] is extended here to the three bulk elastic

DOI: 10.1021/acs.macromol.8b00900
Macromolecules 2018, 51, 5409−5419

constants (i.e., splay, twist, and bend). The theoretical approach, despite the drawback of some unavoidable approximation, has the advantage of a lower computational cost; therefore, it has been used for more extensive investigation of the phase diagram. Moreover, theory is useful to disentangle the special features coming from flexibility and self-assembly. The phase behavior and the elastic properties of our model system are consistent with experimental findings for SSY. Remarkably, the elastic constants are highly anisotropic, a result that we explain considering the average value and distribution of contour lengths and the persistence length of aggregates.

The paper is organized as follows: the next section presents the model, together with details of the Monte Carlo (MC) simulations and an outline of the Onsager-like theoretical approach. In the third section we show the results of simulations and theory, and finally in the fourth section we draw our conclusions.

METHODS

Model. Our model system is composed of hard disks as those shown in Figure 1, with aspect ratio $X_0 = \mathcal{L}_d/D = 0.31$, where D is the diameter and $\mathcal{L}_d$ is the thickness of a disk. Each disk is decorated with two attractive sites on its bases, which are located along the symmetry axis, at a distance $\mathcal{L}_d/2 + 0.164D$ from the center of mass. Sites belonging to distinct particles interact via a square-well (SW) potential; i.e., $u_{SW} = -u_0$ if $r \le \delta$ and $u_{SW} = 0$ if $r > \delta$, where r is the distance between interacting sites, $\delta = 0.273D$ is the interaction range (which corresponds to the diameter of the yellow spheres in Figure 1), and u_0 is the binding energy. In our model u_0 does not depend on the aggregate size, i.e., aggregation is isodesmic.[40] The binding energy is used to define the temperature scale, i.e., $T^* = k_BT/u_0$.

The disk aspect ratio has been inspired by the shape of the SSY molecule,[32] whereas patch position and size (i.e., distance along symmetry axis and δ) ensure that (i) no branching occurs in the system and that (ii) the (dimensionless) persistence length l_p of aggregates (calculated as in ref 38) is equal to 22.9 disks, a value consistent with the estimate provided in ref 14. Note that this value is independent of temperature and volume fraction as discussed in ref 38.

Monte Carlo Simulations. We used standard isothermal–isobaric (NPT) and canonical (NTV) MC simulations to evaluate the equation of state and to estimate elastic constants, respectively. In NPT-MC simulations we studied 1000 disks in a cubic box of side L with periodic boundary conditions for the following scaled temperatures T^*: 0.09, 0.10, and 0.11. NPT simulations lasted at least 2×10^8 MC steps, and the equation of state was evaluated during the final 5×10^7 MC steps. *NTV* simulations were carried out using $N = 8000$ particles and lasted at least 3×10^6 steps, and elastic constants were evaluated during the final 2×10^6 steps. The nematic order parameter S was determined as the largest eigenvalue of the ordering tensor, calculated as in ref 47. Elastic constants were obtained from the fluctuations of the nematic director as proposed by Allen and Frenkel.[48−51]

Theory. The Helmholtz free energy F of the N phase formed by a polydisperse mixture of self-assembling linear aggregates is expressed as a functional of the number density of aggregates $\nu(l)$. Here l is the length (or number of monomers) of the aggregate to which a monomer belongs. The density function obeys the normalization condition $\sum_l \nu(l) = \rho$, where $\rho = N/V$, with N the number of monomers and V the volume, is the number density of monomers. The Helmholtz free energy of the system can be written as the sum of the following contributions:[38,41,46]

$$F = F^{id} + F^{excl} + F^{or} + F^{st} \tag{5}$$

where F^{id} is the ideal gas free energy and F^{excl} and F^{or} account for the excluded volume interactions and for the entropy decrease due to orientational order, respectively. These three terms represent the Helmholtz free energy in the Onsager theory.[52] The last term, F^{st}, is the stacking free energy, which accounts for monomer aggregation and which is expressed in terms of $\Delta = \Delta(T)$, the bonding free energy.[38] It introduces into the free energy a nontrivial dependence on temperature, through the length distribution $\nu(l)$. Here, we have assumed for F^{st} the same functional form that was obtained in ref 40, and an exponential aggregate length distribution is assumed, i.e. $\nu(l) = \rho M^{(l-1)}/(M-1)^{(l+1)}$, with M the average number of disks in an aggregate.[38]

Nematic–Isotropic Phase Transition. The F^{or} contribution to the free energy is given by the product of temperature times an entropic term, which vanishes in the isotropic phase. Two expressions were proposed for the limiting cases of stiff (A) and very flexible (B) chains.[53] For our system, F^{or} is expressed as the sum of contributions having the A (B) form for aggregates shorter (longer) than a reference value l_0,[38] which is an adjustable parameter of the order of the persistence length l_p; in the present case, using the same procedure discussed in ref 38, $l_0 \approx 27$ was found.

The excluded volume contribution to the free energy in the absence of deformation, F_0^{excl}, is expressed as

$$\frac{\beta F_0^{excl}}{V} = \frac{\eta(\Phi)}{2} \sum_l \sum_{l'} \nu(l)\nu(l')\bar{v}^{excl}(l, l') \tag{6}$$

where $\bar{v}^{excl}(l,l')$ is the average excluded volume between two aggregates made of l and l' disks and $\eta(\Phi)$ is the Parsons–Lee factor,[54,55] introduced to account for higher order terms in the virial expansion. Here Φ is the effective volume fraction, i.e. $\Phi = \xi\phi$, with ξ a scaling factor whose meaning will be discussed later and ϕ volume fraction of disks. Concerning the average excluded volume $\bar{v}^{excl}$, let us consider two chains, 1 and 2, composed of l and l' monomers. If $\mathbf{R}_1 = \{\mathbf{r}_{1,1}...\mathbf{r}_{1,l}\}$, $\mathbf{R}_2 = \{\mathbf{r}_{2,1}...\mathbf{r}_{2,l'}\}$, $\mathbf{U}_1 = \{\mathbf{u}_{1,1}...\mathbf{u}_{1,l}\}$, and $\mathbf{U}_2 = \{\mathbf{u}_{2,1}...\mathbf{u}_{2,l'}\}$, where $\mathbf{r}_{\gamma,i}$ and $\mathbf{u}_{\gamma,i}$ are the position and the orientation (unit vector) of monomer i belonging to chain $\gamma = 1, 2$, the average excluded volume in the isotropic phase is defined as

$$\bar{v}_{iso}^{excl}(l, l') = -\frac{1}{16\pi^2 V^{l+l'-1}} \int' d\mathbf{R}_1\, d\mathbf{R}_2\, d\mathbf{\Omega}_1\, d\mathbf{\Omega}_2 \times e_{12}^{ll'}(\mathbf{R}_1, \mathbf{U}_1, \mathbf{R}_2, \mathbf{U}_2) \tag{7}$$

where $d\mathbf{R}_\gamma = \prod_{i=1}^{l} d\mathbf{r}_{\gamma,i}$ and $d\mathbf{\Omega}_\gamma = \prod_{i=1}^{l} d\boldsymbol{\omega}_{\gamma,i}$ with $d\boldsymbol{\omega}_{\gamma,i}$ the infinitesimal solid angle around the orientation $\mathbf{u}_{\gamma,i}$ and $e_{12}^{ll'}$ is the Mayer function:[56]

$$e_{12}^{ll'}(\mathbf{R}_1, \mathbf{U}_1, \mathbf{R}_2, \mathbf{U}_2) = \exp\{-U_h(\mathbf{R}_1, \mathbf{U}_1, \mathbf{R}_2, \mathbf{U}_2)/k_BT\} - 1 \tag{8}$$

with $U_h(\mathbf{R}_1,\mathbf{U}_1,\mathbf{R}_1,\mathbf{U}_2)$ being the hard-core pair potential:

$$U_h(\mathbf{R}_1, \mathbf{U}_1, \mathbf{R}_2, \mathbf{U}_2) = \begin{cases} \infty & \text{if 1, 2 overlap} \\ 0 & \text{if 1, 2 do not overlap} \end{cases} \tag{9}$$

The prime in the integral of eq 7 means that it has to be evaluated over all positions and orientations of monomers such that (i) within each chain only two monomers are single bonded and all the remaining monomers (if any) are double bonded[a] and that (ii) chains do not self-overlap.

The average excluded volume in the isotropic phase is calculated by Monte Carlo integration of eq 7 for $l, l' \le 10$. Then, the numerical values are fit to an analytical form (see Supporting Information), which corresponds to the Onsager expression[52] for the excluded volume of two hard cylinders of diameter of diameter D and lengths $\xi X_0 Dl$ and $\xi X_0 Dl'$, where ξ is a factor accounting for the fact that because of the finite range of SW interaction between patches, the length of an aggregate is not simply the sum of disk lengths.

The average excluded volumes in the nematic phase are different from those in the isotropic phase because the orientational distribution function has changed. We have assumed the Onsager orientational distribution function:[52]

$$f_O(\mathbf{u}) = \frac{\alpha}{4\pi \sinh \alpha} \cosh(\alpha \cos\theta) \tag{10}$$

DOI: 10.1021/acs.macromol.8b00900
Macromolecules 2018, 51, 5409−5419

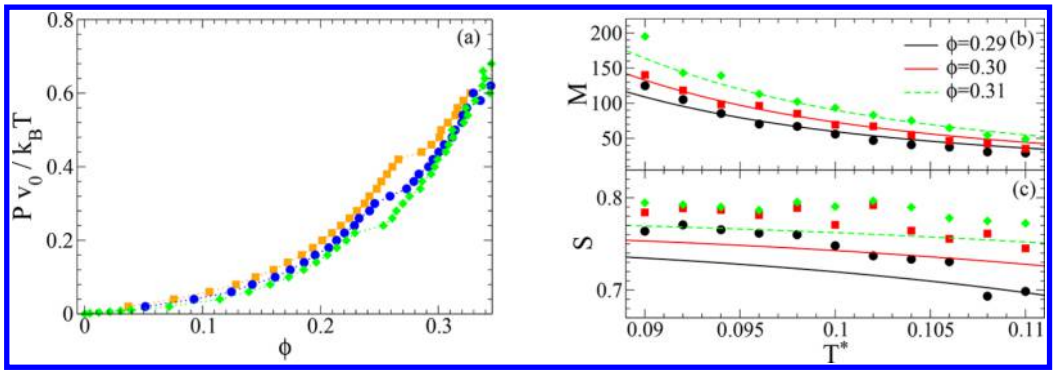

Figure 2. (a) Equation of state obtained from MC simulations at different temperatures, $T^* = 0.09$ (green), 0.10 (blue), and 0.11 (orange). Pv_0/k_BT, with v_0 the volume of a disk, is the dimensionless pressure. (b) Average aggregate length M and (c) nematic order parameter S as a function of temperature for volume fraction of disks $\phi = 0.29$, 0.30, and 0.31. Symbols are numerical estimates from MC simulations, and solid lines are theory predictions.

where θ is angle between the particle orientation $\mathbf{u}$ and the nematic director and α is a non-negative parameter, which increases with increasing order. The parameter α is related to the nematic order parameter S as

$$S = \int_0^\pi \mathrm{d}\theta \sin\theta \left(\frac{3}{2}\cos^2\theta - \frac{1}{2}\right) f_O(\cos\theta) = 1 - 3\frac{\coth\alpha}{\alpha} + \frac{3}{\alpha^2} \xrightarrow{\text{high } \alpha} 1 - \frac{3}{\alpha} \tag{11}$$

Then, the average excluded volumes in the nematic phase are calculated using the form of the average excluded volume between two cylinders adopted in ref 38, which is a function of the parameter α (see eq S.2 in the Supporting Information).

The analytical forms of the average excluded volume in the isotropic and in the nematic phase are used for arbitrary lengths in eq 6. The total free energy, eq 5, is expressed as a function of the average aggregate length M and of the orientational parameter α, whose values at a given volume fraction and temperature are obtained by minimizing the free energy. Coexistence lines are built using the condition of equal pressure and chemical potential in the isotropic and in the nematic phase.

Elastic Constants. Starting from a microscopic expression for the Helmholtz free energy, such as eq 5, the elastic constants for a system of low molar mass nematics can be easily obtained, under the assumption that the local free energy density in a deformed sample remains the same as in the absence of deformation, but with respect to the local director. This assumption is justified by the large length scale of director deformations compared to the molecular size. Thus, in eq 5 only the excluded volume contribution, F^{excl}, is affected by the distortion. By truncating the Taylor expansion of F^{excl} with respect to director displacements, we can write

$$\frac{F^{\mathrm{excl}}}{V} = \frac{F_0^{\mathrm{excl}}}{V} + \frac{q_1^2}{2}K_{11} + \frac{q_2^2}{2}K_{22} + \frac{q_3^2}{2}K_{33} \tag{12}$$

where F_0^{excl} is the excluded volume contribution to the free energy of the undeformed nematic phase, q is the wavelength of the distortion, and K_{11}, K_{22}, and K_{33} are the splay, twist, and bend elastic constants, respectively. These are expressed in terms of integrals analogous in form to eq 7, with a different integrand.[57]

In the case of semiflexible polymers, the need of analyzing the configurational statistics in a space-dependent nematic field makes the development of an elastic theory a formidable task. Here, we use an approximate treatment, where segments shorter than l_0 are treated as rigid, while those longer than or equal to l_0 are decomposed into effective rigid segments of length l_0.[31] Thus, for a mixture of aggregates of different lengths, the elastic constants K_{ii} ($i = 1, 2, 3$) are calculated as

$$K_{ii} = \frac{k_BT\eta(\Phi)}{2}\left\{\sum_{l=1}^{l_0-1}\sum_{l'=1}^{l_0-1}\nu(l)\nu(l')\overline{v}_{ii}^{\mathrm{excl}}(l, l') + 2\sum_{l=1}^{l_0-1}\sum_{l'\geq l_0}\nu(l)\nu(l')\frac{l'}{l_0}\overline{v}_{ii}^{\mathrm{excl}}(l, l_0) + \sum_{l\geq l_0}\sum_{l'\geq l_0}\nu(l)\nu(l')\frac{ll'}{l_0^2}\overline{v}_{ii}^{\mathrm{excl}}(l_0, l_0)\right\} \tag{13}$$

where $\overline{v}_{ii}^{\mathrm{excl}}(l,l')$ is the average generalized excluded volume between two aggregates made of l and l' disks. This is evaluated as

$$\overline{v}_{ii}^{\mathrm{excl}}(l, l') = -\frac{1}{V^{l+l'-1}}\int' (R_{\mathrm{cm}}^i)^2 e_{12}^{ll'}(\mathbf{R}_1, \mathbf{u}_1, \mathbf{R}_2, \mathbf{u}_2)(\mathbf{u}_1\cdot\hat{\mathbf{X}})(\mathbf{u}_2\cdot\hat{\mathbf{X}}) \times \dot{f}_O(\mathbf{u}_1)\dot{f}_O(\mathbf{u}_2)\,\mathrm{d}\mathbf{R}_1\,\mathrm{d}\mathbf{R}_2\,\mathrm{d}\omega_1\,\mathrm{d}\omega_2 \tag{14}$$

where all monomers belonging to aggregate γ have the same orientation $\mathbf{u}_\gamma$, R_{cm}^i is a Cartesian component of $\mathbf{R}_{\mathrm{cm}} = (X_{\mathrm{cm}}, Y_{\mathrm{cm}}, Z_{\mathrm{cm}})$, which is the center-of-mass position of aggregate 2 relative to aggregate 1 in a reference frame (X, Y, Z) with Z parallel to the local director at the position of particle 1 (R_{cm}^i equal to X_{cm} for $i = 1$, Y_{cm} for $i = 2$, Z_{cm} for $i = 3$), $\hat{\mathbf{X}}$ is the unit vector parallel to the X-axis, and f_O is the first derivative of the Onsager orientational distribution function with respect to its argument. The generalized excluded volumes $\overline{v}_{ii}^{\mathrm{excl}}(l,l')$ are estimated through Monte Carlo integration of eq 14 and then numerical data are fit to analytical forms (see eq S.6 in the Supporting Information).

Additional Cost for Splay Deformation. As mentioned in the Introduction, the cost for splay deformations of polymeric systems has an additional contribution, ΔK_{11}, which originates from the coupling between director field and areal density.[30,58] Thus, we express the renormalized splay elastic constant as

$$K_{11} = K_{11}^0 + \Delta K_{11} \tag{15}$$

where K_{11}^0 is the bare splay constant (eq 13). Extending to the a polydisperse mixture of aggregates the expression for the decrease of entropy caused by the splay deformation, under the assumption that polymer ends are randomly distributed as in an ideal gas,[58] we can write

$$\frac{\Delta K_{11}}{k_BT} = \frac{F(\alpha)^2}{2}\sum_l l^2\nu(l) \tag{16}$$

where $DX_0lF(\alpha)$ is the average projection of the length of an aggregate of l monomers along the nematic director. Using the relationship

$$\sum_l l^2\nu(l) = \rho(2M - 1) \tag{17}$$

DOI: 10.1021/acs.macromol.8b00900
Macromolecules 2018, 51, 5409−5419

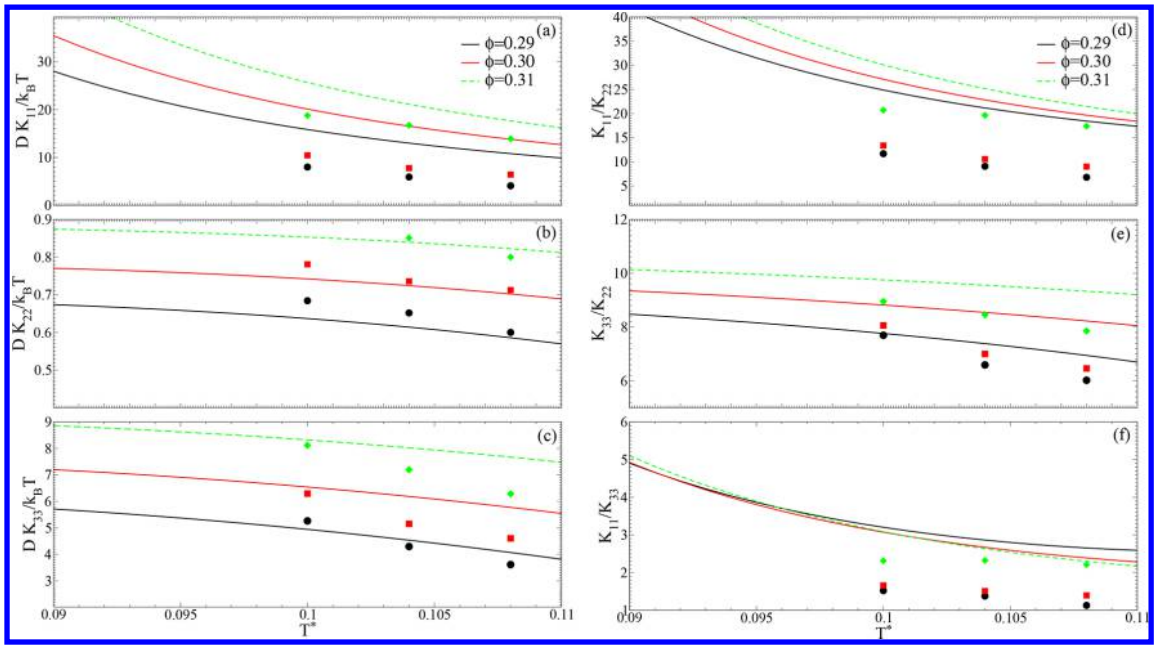

Figure 3. Dimensionless elastic constants (a–c) and elastic ratios (d–f) obtained from MC simulations (symbols), as a function of temperature, for volume fraction of disks ϕ = 0.29 (black), 0.30 (red), and 0.31 (green). The lines show the results of theory. D is the diameter of a disk.

eq 16 becomes

$$\frac{\Delta K_{11}}{k_B T} = \frac{F(\alpha)^2}{2}\rho(2M - 1) \tag{18}$$

The factor $F(\alpha)$ is estimated through Monte Carlo integration, as outlined in the Supporting Information.

RESULTS AND DISCUSSION

Monte Carlo Simulations. Figure 2a shows the equation of state obtained from MC simulations at T^* = 0.09, 0.10, and 0.11. In this figure ϕ is the volume fraction of disks, calculated as $\phi = Nv_0/L^3$, where N is the number of disks in the system, L is the side of the cubic box, and $v_0 = \pi X_0 D^3/4$ is the volume of a disk.

The temperature range corresponds to the region investigated in ref 59, assuming a bonding energy of linear aggregates, u_0, equal to 10 k_BT, which is in line with the estimate of 7–11 k_BT reported in the literature for SSY.[14,60] In the equation of state we can distinguish an isotropic and a nematic branch at larger volume fraction, with the phase transition shifted at higher ϕ values as temperature increases.

Figures 2b,c show the temperature dependence of the average aggregation number, M, and of the nematic order parameter, S, for volume fractions in the nematic range. The average aggregation number increases with decreasing temperature and with increasing concentration, reaching values of the order of hundreds at the lowest T^* values. Hence, the average aspect ratios of aggregates can be estimated between around 20 and more than 50. Such values are considerably higher than the experimental values obtained for SSY from correlation lengths measured in SAXS experiments, which range between 10 and 14.[59,61] However, it was pointed out that such estimates are hard to reconcile with the formation of the nematic phase,[59] and indeed larger values, from tens to hundreds of monomer units, which are in better agreement with the results of our simulations, were inferred from NMR measurements of diffusion coefficient in the isotropic phase.[60]

Figure 2c shows the orientational order parameter S, calculated from the orientation of the normals to disks. It increases with increasing volume fraction, as expected for lyotropic polymers. Additionally, the order parameter shows here a significant increase with lowering temperature, as in thermotropic liquid crystals, although the S values are much higher than for typical thermotropic nematics. Concentration and temperature dependence of the order parameter shown in Figure 2c are analogous to the typical experimental data exhibited by chromonics. The data available in the literature for SSY show some dispersion: using polarized Raman spectroscopy, S values between 0.7 and 0.85 were obtained,[62,63] whereas lower values, in the range 0.6–0.75, were determined by UV–vis absorption spectroscopy,[42] and even lower values were inferred from NMR spectroscopy (0.54–0.65)[44] and birefringence measurements (≃0.52–≃0.63).[14] The origin of the temperature dependence of the order parameter in chromonics is not obvious: it may reflect the presence of interaggregate interactions other than pure excluded volume repulsion as well as the temperature dependence of the aggregate length.[43] In our simulations, due to the hard-core nature of the interactions between aggregates, only the latter can be responsible for the behavior shown in Figure 2c; the increase of S with decreasing temperature is a signature of molecular self-assembly and derives from the increase in length of aggregates. In principle, also the change of the persistence length l_p could affect the orientational order parameter, but this is not the case of our simulations, since in our coarse-grained model the persistence length l_p of aggregates is independent of T and ϕ. The calculated order parameters are high, close to the data obtained by polarized Raman spectroscopy,[63] although the sensitivity to temperature seems weaker than in experimental data. This is presumably due to the form of the interaction potential in our coarse-grained model. Better agreement with experiments could be achieved by a more realistic modeling of monomers stacking interaction. Stacking forces are supposed to originate

DOI: 10.1021/acs.macromol.8b00900
Macromolecules 2018, 51, 5409–5419

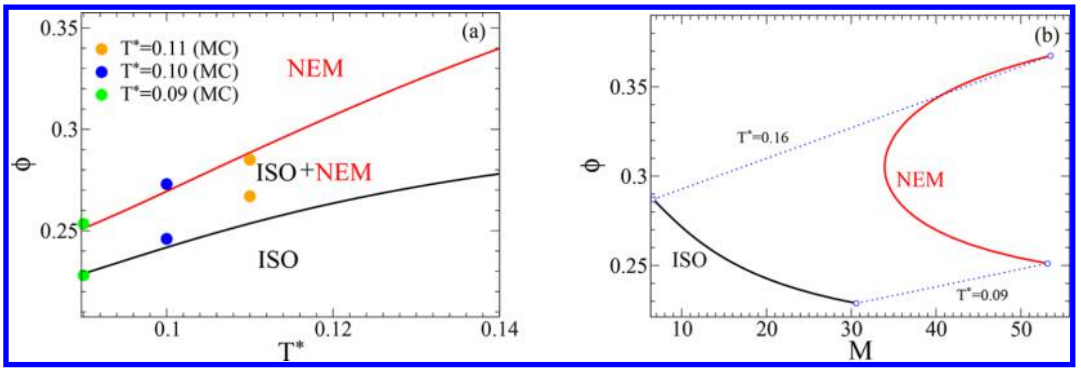

Figure 4. (a) Theoretical phase diagram (lines), with symbols showing numerical estimates of phase boundaries obtained from MC simulations. ϕ is the volume fraction of disks, and T^* is the dimensionless temperature. (b) Isotropic−nematic coexistence lines in the average aggregation number M and volume fraction, ϕ, plane. The dotted lines connect points corresponding to the isotropic and to the nematic phase in equilibrium at a given temperature.

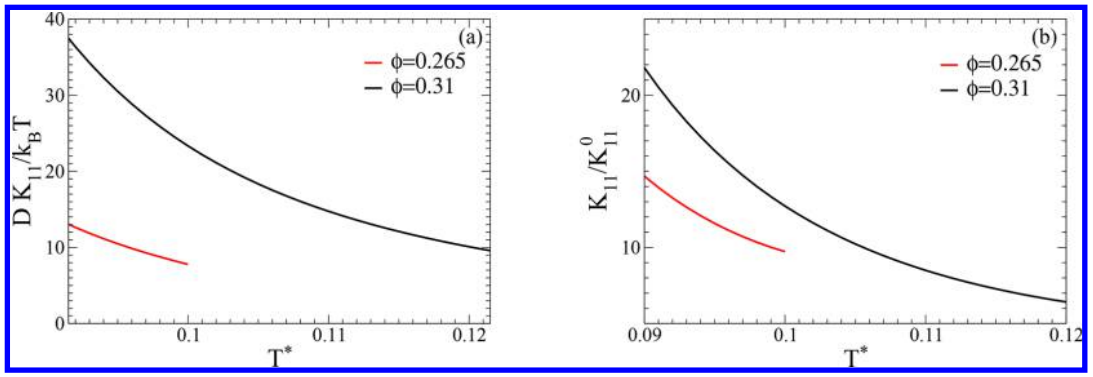

Figure 5. (a) Dimensionless splay elastic constant K_{11} and (b) ratio of the renormalized to the bare splay constant, K_{11}/K_{11}^0, as a function of temperature for volume fractions of disks ϕ = 0.265 and ϕ = 0.31. D is the diameter of a disk.

from hydrophobic effect which is expected to exhibit a strong temperature dependence.[64]

The plots in Figure 3 show the elastic constants and their ratios as a function of temperature at different concentrations. The splay constant obtained from the analysis of director fluctuations contains both contributions appearing in eq 15. We can see that the elastic constants have the same order of magnitude as experimental data for chromonics.[14−15] The twist elastic constant is an order of magnitude lower than both bend and splay constants, with the splay nearly twice as big as the bend. This is different from the typical behavior of conventional low molar mass thermotropic liquid crystals, which also exhibit K_{22} smaller than K_{11} and K_{33}, but with K_{33}/K_{22} that rarely exceeds 2 or 3 and K_{33}/K_{11} generally larger than 1. High elastic anisotropy is characteristic of polymer liquid crystals. For thermotropic polymers, K_{11} orders of magnitude larger than K_{33} was reported.[22,23] The available data for lyotropic polymers show a wide variability of the K_{11}/K_{33} ratio, ranging from values of the order of 0.1 for colloidal suspensions of stiff TMV[24,25] to values of the order of 1 (either smaller or larger than 1) for solutions of the more flexible PBG,[26] for which however also ratios as high as 1000 can be found.[27] Experimental data for chromonics are comparable with those for PBG: $K_{33}/K_{22} \sim 10$ and $K_{33}/K_{11} \sim 1$ for SSY;[14] $K_{33}/K_{22} \sim 35$ and K_{33}/K_{11} between 1 and 2 for DSCG.[16]

Figure 3 shows that all three elastic constants decrease with increasing temperature and decreasing volume fraction, in qualitative agreement with experiments on chromonics[14,16] and also in agreement with experiment is the temperature and concentration dependence of the elastic ratios, K_{33}/K_{22}, K_{11}/K_{22}, and K_{11}/K_{33}. Especially significant is the temperature dependence of the elastic ratios on temperature, which cannot be explained by the theory for semiflexible rods of fixed length.

Comparing with the experimental data for SSY,[14] we can see that the calculated elastic constants are too high, especially the splay one, which exhibits also a too weak temperature dependence. On the other end, the ratios K_{33}/K_{22} are close to experimental values, whereas elastic ratios involving K_{11} are overestimated. These results, together with the high and rather weakly temperature-dependent order parameter, suggest that the average length of aggregates may be overestimated. Better agreement could be achieved by tuning the geometry and energetic parameters of the model, which affect the contour and persistence lengths of aggregates, but this is beyond the scope of the present work.

Theory. Figure 4a shows the theoretical phase diagram, together with estimates of phase boundaries from MC simulations for T^* = 0.09, 0.10, and 0.11. Isotropic−nematic coexistence is found at a volume fraction of disks, ϕ, roughly in the range 0.25−0.34. The upper limit could be overestimated because the columnar phase, which is not accounted for by the present theoretical treatment, might override the nematic phase at high densities. The results of theory are in reasonable agreement with those of MC simulations, whereas comparison with experimental data for SSY[59] shows that the volume fraction of the isotropic−nematic coexistence region is too high. However, there is some ambiguity in the experimental determination of volume fractions, and different evaluations can be found in the literature (see, e.g., refs 15, 42, and 59 and the Supporting Information of ref 14). Another issue that

DOI: 10.1021/acs.macromol.8b00900
Macromolecules 2018, 51, 5409−5419

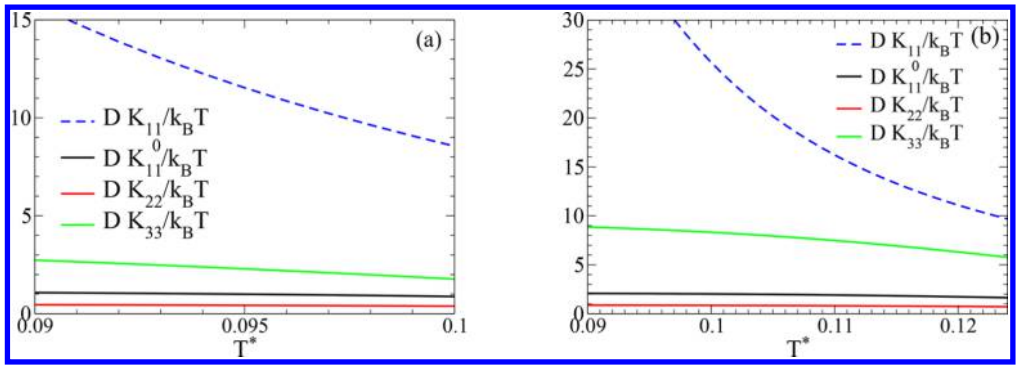

Figure 6. Dimensionless elastic constants as a function of temperature from $T^* = 0.09$ up to isotropic−nematic coexistence at the volume fractions of disks (a) $\phi = 0.265$ and (b) $\phi = 0.31$. D is the diameter of a disk.

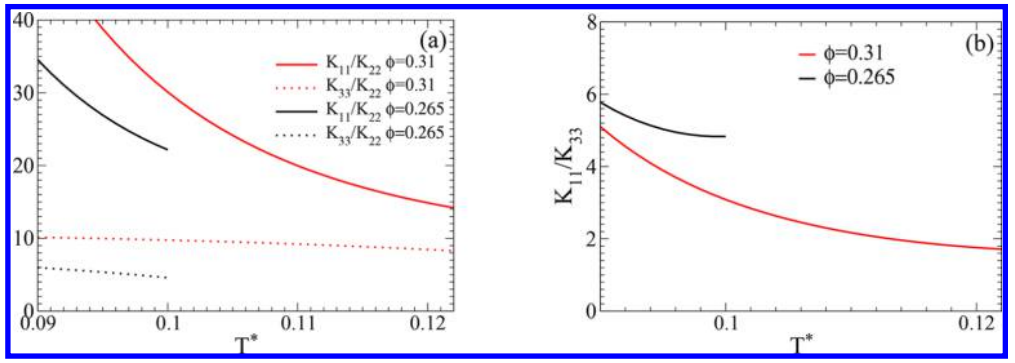

Figure 7. Temperature and concentration dependence of the elastic ratios (a) K_{11}/K_{22}, K_{33}/K_{22} and (b) K_{11}/K_{33} at different values of the volume fraction of disks ϕ.

comes into play when comparing our calculated volume fractions with experimental data is that chromonic molecules have two ionizable sulfonate groups at their surface. These (partially) unscreened charges originate additional electrostatic repulsion between aggregates, beside the steric repulsion present in our model, which could be accounted for through an effective diameter, larger than the steric one. Assuming a Debye screening length around 0.3 nm, as reported in the experiments described in ref 14, we can estimate an effective volume of aggregates that is about 1.7 times the steric one. Dividing our volume fractions by this factor, we obtain values that are very close to the experimental ones.

In Figure 4b the theoretically estimated coexistence lines in the $M-\phi$ plane show a re-entrant behavior, as already observed in past studies of the phase diagrams for DNA oligomers.[38,40] We note that theoretical results suggest that in the nematic phase the average aggregation number M cannot be lower than 30−32 monomer units. The average length of aggregates exhibits a minimum along the nematic coexistence line, a theoretical prediction that still awaits experimental confirmation. In Figures 2b,c the theoretical estimates of the average aggregation number M and order parameter S at $\phi = 0.29$, 0.30, and 0.31 are compared with the results of MC simulations. The value of M is quite well captured by theoretical calculations, while the theoretical order parameters are generally lower than the simulation values.

Figure 5a shows the renormalized elastic constant K_{11}, eq 15, as a function of temperature for the volume fraction of disks $\phi = 0.265$ and 0.31. K_{11} increases with decreasing temperature and increasing concentration. From Figure 5b, which displays the ratio K_{11}/K_{11}^0 as a function of temperature, for the same concentrations as in Figure 5a, we can infer that the main contribution to K_{11} comes from ΔK_{11}. The relative weight of ΔK_{11} strongly increases with increasing concentration and lowering temperature, and the bare splay constant gives a non-negligible contribution only at high temperature and low concentration. This can be explained considering that $\Delta K_{11} \propto M(\phi,T)$ (see eq 18 and Figure 2b). A dominant role of ΔK_{11} is expected for long polymers,[29,31] and in a recent Monte Carlo study of a thermotropic polymer with contour length much longer (up to an order of magnitude) than the persistence length, it was found that the cost for splay deformation could be essentially ascribed to ΔK_{11}.[65] Our case is different, because neither of the two contributions to the splay elastic constant seems to be negligible. This suggests that the interplay of these contributions could be a relevant aspect of the elastic behavior of chromonics, which has not been pointed out yet.

The twist and bend elastic constants, K_{22} and K_{33}, as well as the bare splay constant, K_{11}^0, depend on the persistence length of aggregates; therefore, they are expected to saturate to a limiting value on lowering the temperature and increasing concentration (cf. eq 13). This behavior is shown in Figure 6, which reports all the elastic constants as a function of temperature up to coexistence, for two different values of the disk volume fraction, namely $\phi = 0.265$ and 0.31. Consistently with the results of MC simulations, shown in Figure 3a−c, and with experimental results for SSY[14] and for DSCG,[16] theoretical estimates of elastic constants decrease on increasing temperature and on lowering concentration. Comparing with the results of MC simulations (Figure 3), we can see that theoretical predictions for K_{22} and K_{33} are close to the numerical results, although their temperature dependence seems to be underestimated. On the contrary, K_{11} is significantly larger than numerical values, which suggests that

DOI: 10.1021/acs.macromol.8b00900
Macromolecules 2018, 51, 5409−5419

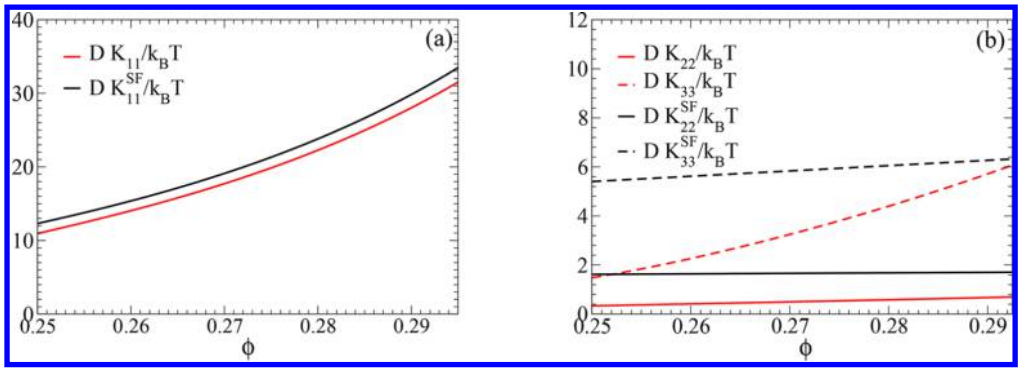

Figure 8. Splay (a) and twist and bend (b) dimensionless elastic constants calculated at $T^* = 0.09$ using the present theory and the expressions for semiflexible polymers (SF), eqs 2−4, as a function of the disk volume fraction ϕ. D is the diameter of a disk.

eq 18 provides a crude estimate of ΔK_{11} and needs to be improved.

At the lower concentration (see Figure 6a) the bend elastic constant K_{33} is much smaller than the renormalized splay constant K_{11} at any temperature. The two constants become comparable at higher temperatures and concentrations. Anyway, both K_{11} and K_{33} are always much greater than K_{22}. This behavior is clearer in Figure 7, which shows the relative values K_{11}/K_{22}, K_{33}/K_{22} (a) and K_{11}/K_{33} (b) at two different densities. The trends are analogous to those reported in recent experimental studies of chromonics.[14,16]

Comparison with the results of MC simulations, reported in Figure 3e, shows rather good agreement for K_{33}/K_{22}, although theory underestimates the temperature dependence of this ratio. The comparison is less satisfactory in the case of elastic ratios involving the splay constant, which can be ascribed to the lower quality of ΔK_{11} predictions. We can see that both K_{11}/K_{22} and K_{11}/K_{33} (see Figures 3d and 3f, respectively) are higher than the numerical results and their sensitivity to changes in concentration is strongly underestimated. Moreover, K_{11}/K_{33} is predicted to decrease with increasing density, whereas in MC simulations it is found to increase, in agreement with measurements[14] and experimental findings[5] for SSY.

It is now interesting to compare our results with those obtained using eqs 2−4 for semiflexible polymers of fixed contour length. The persistence length is calculated as $\lambda_p = \xi X_0 D l_p$, so it is assumed to be constant at any temperature and density. On the other end, the average aggregate length is calculated from the average number of disks in aggregates M as $\mathcal{L} = \xi X_0 D M(\phi, T^*)$; therefore, it depends on temperature and density. Figure 8 shows the elastic constants as a function of the volume fraction, at the temperature $T^* = 0.09$. We can see that K_{11} and K_{11}^{SF} are similar, the reason being that K_{11} is dominated by the nonexcluded volume contribution, ΔK_{11}, which according to eq 18 depends on the average length of aggregates, analogously to eq 2. On the contrary, there are significant relative differences between the two estimates of the twist constant, K_{22} and K_{22}^{SF}, and of the bend constant, K_{33} and K_{33}^{SF}. The differences concern the magnitude and the density dependence: both elastic constants obtained from our calculations are smaller and more sensitive to changes in density than the corresponding quantities calculated according to eqs 2. Density affects K_{22} and K_{33} through the length distribution of aggregates, which includes values shorter and longer than the persistence length, and through the degree of orientational order. The former is not accounted for by eq 2, whereas the latter is included in the asymptotic limit of very high ordering.[31]

Comparison with Experiments in Confined Systems. The unconventional elasticity of chromonics is evidenced by unusual phenomenologies in confined systems, which have been interpreted as a signature of high elastic anisotropy, i.e., $K_{33}, K_{11} \gg K_{22}$. One of these is the emergence of twisted director configurations (both right- and left-handed) in spherical droplets of SSY in oil[5] and in tactoids of DSCG,[3] i.e., spindle-shaped nematic nuclei that form upon cooling the isotropic phase. This is an amazing example of chiral symmetry breaking, since chiral structures appear in the absence of molecular chirality in the systems. Twisted director patterns were observed, in certain temperature ranges, also in tangentially anchored spherical droplets of low molar mass thermotropic nematics.[66,67] They were predicted to appear when the following disequality holds:[68]

$$K_{33}/K_{11} \leq 2.32(1 - K_{22}/K_{11}) \tag{19}$$

which requires small K_{22}/K_{11} and/or K_{33}/K_{11}. It can be easily seen that these conditions are satisfied by the elastic constants reported in Figures 3 and 5−7 and that crucial to this purpose is the role of the nonexcluded volume contribution to the splay constant, ΔK_{11}.

A more subtle effect was investigated in ref 63, where tactoids of SSY were found to change from a bipolar to a twisted bipolar and finally to a new splay-minimizing configuration with lowering concentration. It was proposed that this behavior would reflect the relative increase in length of aggregates with decreasing density, along the isotropic−nematic coexistence. This would lead to a strong increase of the splay elastic constant, which depends on the aggregate length, and would have much lower effect on the bend and twist moduli, which are essentially determined by the persistence length of aggregates. Our theoretical predictions show that indeed the ratio K_{33}/K_{11} decreases as the coexistence concentration decreases, but this is due to the contribution of both the splay and the bend elastic constant. We have seen that the splay elastic constant is dominated by the nonexcluded volume contribution ΔK_{11}, and according to eq 18, $\Delta K_{11}/\phi$ is proportional to the average aggregate length M, which increases with decreasing density (Figure 4b below $\phi \approx 0.31$). At the same time K_{33}/ϕ decreases, and the same does K_{22}/ϕ, although to a lesser extent (see e.g., Figure 6), which is not predicted by eqs 3 and 4, at least if the persistence length is constant. Figure 9 shows the terms on the two sides of eq 19 along the isotropic−nematic coexistence, and we can see that

DOI: 10.1021/acs.macromol.8b00900
Macromolecules 2018, 51, 5409−5419

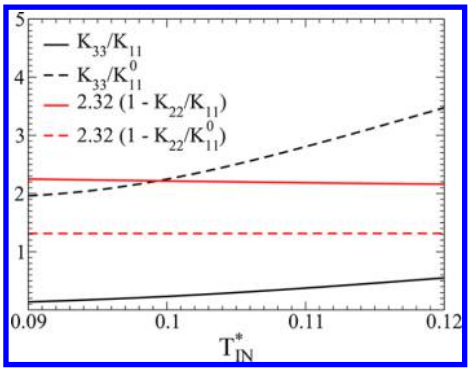

Figure 9. Behavior of the terms on the two sides of eq 19 as a function of temperature (T_{IN}^*), along the nematic−isotropic coexistence line (i.e., red line in Figure 4a). K_{11}^0 is the bare splay constant, determined by the excluded volume.

the inequality is always satisfied, which means that at any concentration a twisted director configuration is predicted. Interestingly the opposite, i.e., a bipolar droplet configuration at any concentration, would be obtained if the bare splay constant, K_{11}^0, had been used, as shown by the dashed lines in Figure 9. This suggests that the nonexcluded volume contribution to the splay elastic constant, ΔK_{11}, has a subtle role for the change of tactoid configuration reported in ref 63 and that the expression that we used in eq 18 has to be improved.

CONCLUSIONS

Stimulated by evidence of unconventional behavior, which has been reported for chromonic liquid crystals, we have investigated the elastic properties of the nematic phase of a system of hard patchy disks undergoing reversible polymerization. We have used Monte Carlo simulations and a theoretical approach based on Onsager theory, which takes into account the formation of polydisperse linear aggregates and includes an approximate treatment of the flexibility of aggregates. To our knowledge, the elastic properties of self-assembly driven nematics were not previously investigated by theory or simulations, with a single recent exception of Monte Carlo simulations.[39] These however could not provide new useful insights, since the calculated elastic properties did not show the distinctive features exhibited by chromonics. On the contrary, such features emerge from our study, and we can identify the effects of molecular self-assembly, which controls the average value and distribution of aggregate lengths, and those of the intrinsic flexibility of aggregates. The support of theory helps to rationalize the results of MC simulations.

The systems of polymerizing disks investigated here, using parameters suitable for chromonics, contain a mixture of aggregates with sizes ranging from less than the persistence length up to 7−8 times the persistence length. Their contributions to the elastic constants do not scale in a trivial way with size, but reflect different behaviors, between the limiting cases of rigid rods and long semiflexible polymers. The interplay of length distribution and intrinsic flexibility are the main factors affecting the twist and bend elastic constants. The splay constant differs from the other two because, besides the excluded volume term, there is an additional term deriving from the coupling between director field and areal density (ΔK_{11}), whose relative weight depends on the ratio between persistence and contour length. This term generally overcomes the excluded volume contribution, but unlike what occurs for very long polymers,[65] it is not an order of magnitude larger. Our results suggest that the simultaneous presence of the two contributions to the splay constant is one important reason behind the special elastic behavior of chromonics.[14,16]

The elastic constants that we calculate show specific features exhibited by chromonics; i.e., they increase both when concentration increases and when temperature decreases. This temperature dependence is absent for hard polymers and it is a consequence of molecular self-assembly. On the basis of our results, we can analyze some puzzling behaviors that were recently reported for chromonics under confinement. The high values of K_{11}/K_{33} and K_{11}/K_{22} are in agreement with the formation of spontaneously twisted director configurations. Moreover, we can discuss the origin of changes in director configuration, which were observed in tactoids on moving along the nematic−isotropic coexistence. Again, a key role of the nonexcluded volume contribution to the splay elastic constant, ΔK_{11}, emerges, and the comparison with experimental data shows that the simple form that we have used, based on the assumption that polymer ends are randomly distributed as in an ideal gas, has to be improved to reach a more quantitative agreement.

ASSOCIATED CONTENT

Supporting Information

The Supporting Information is available free of charge on the ACS Publications website at DOI: 10.1021/acs.macromol.8b00900.

Some technical aspects of the theory: analytical expressions of the average excluded volumes (isotropic and nematic phases), of the average generalized excluded volumes (elastic constants), and of factor $F(\alpha)$, which enters into the nonexcluded volume contribution to splay elastic constant (PDF)

AUTHOR INFORMATION

Corresponding Authors

*E-mail: alberta.ferrarini@unipd.it (A.F.).
*E-mail: cristiano.demichele@roma1.infn.it (C.D.M.).

ORCID

Alberta Ferrarini: 0000-0001-6211-7202
Cristiano De Michele: 0000-0002-8367-0610

Notes

The authors declare no competing financial interest.

ADDITIONAL NOTE

[a]The only exception is when we have two chains, each of which constituted of two monomers.

REFERENCES

(1) Lydon, J. Chromonic mesophases. *Curr. Opin. Colloid Interface Sci.* **2004**, *8*, 480−490.
(2) Lydon, J. Chromonic review. *J. Mater. Chem.* **2010**, *20*, 10071−10099.
(3) Tortora, L.; Lavrentovich, O. D. Chiral symmetry breaking by spatial confinement in tactoidal droplets of lyotropic chromonic liquid crystals. *Proc. Natl. Acad. Sci. U. S. A.* **2011**, *108*, 5163−5168.
(4) Nych, A.; Ognysta, U.; Musevic, I.; Sec, D.; Ravnik, M.; Zumer, S. Chiral bipolar colloids from nonchiral chromonic liquid crystals. *Phys. Rev. E* **2014**, *89*, 062502.

DOI: 10.1021/acs.macromol.8b00900
Macromolecules 2018, 51, 5409−5419

(5) Jeong, J.; Davidson, Z. S.; Collings, P. J.; Lubensky, T. C.; Yodh, A. G. Chiral symmetry breaking and surface faceting in chromonic liquid crystal droplets with giant elastic anisotropy. *Proc. Natl. Acad. Sci. U. S. A.* **2014**, *111*, 1742−1747.
(6) Jeong, J.; Kang, L.; Davidson, Z. S.; Collings, P. J.; Lubensky, T. C.; Yodh, A. G. Chiral structures from achiral liquid crystals in cylindrical capillaries. *Proc. Natl. Acad. Sci. U. S. A.* **2015**, *112*, E1837−E1844.
(7) Nayani, K.; Chang, R.; Fu, J.; Ellis, P. W.; Fernandez-Nieves, A.; Park, J. O.; Srinivasarao, M. Spontaneous emergence of chirality in achiral lyotropic chromonic liquid crystals confined to cylinders. *Nat. Commun.* **2015**, *6*, 8067.
(8) Zhou, S.; Shiyanovskii, S. V.; Park, H.-S.; Lavrentovich, O. D. Fine structure of the topological defect cores studied for disclinations in lyotropic chromonic liquid crystals. *Nat. Commun.* **2017**, *8*, 14974.
(9) Kumar, A.; Galstian, T.; Pattanayek, S. K.; Rainville, S. The Motility of Bacteria in an Anisotropic Liquid Environment. *Mol. Cryst. Liq. Cryst.* **2013**, *574*, 33−39.
(10) Mushenheim, P. C.; Trivedi, R. R.; Weibel, D. B.; Abbott, N. L. Effects of confinement, surface-induced orientations and strain on dynamical behaviors of bacteria in thin liquid crystalline films. *Biophys. J.* **2014**, *107*, 255−265.
(11) Zhou, S.; Sokolov, A.; Lavrentovich, O. D.; Aranson, I. S. Living liquid crystals. *Proc. Natl. Acad. Sci. U. S. A.* **2014**, *111*, 1265−1270.
(12) Peng, C.; Turiv, T.; Guo, Y.; Wei, Q.-H.; Lavrentovich, O. D. Command of active matter by topological defects and patterns. *Science* **2016**, *354*, 882−885.
(13) Genkin, M. M.; Sokolov, A.; Lavrentovich, O. D.; Aranson, I. S. Topological Defects in a Living Nematic Ensnare Swimming Bacteria. *Phys. Rev. X* **2017**, *7*, 011029.
(14) Zhou, S.; Nastishin, Y. A.; Omelchenko, M. M.; Tortora, L.; Nazarenko, V. G.; Boiko, O. P.; Ostapenko, T.; Hu, T.; Almasan, C. C.; Sprunt, S. N.; Gleeson, J. T.; Lavrentovich, O. D. Elasticity of Lyotropic Chromonic Liquid Crystals Probed by Director Reorientation in a Magnetic Field. *Phys. Rev. Lett.* **2012**, *109*, 037801.
(15) Zhou, S.; Cervenka, A. J.; Lavrentovich, O. D. Ionic-content dependence of viscoelasticity of the lyotropic chromonic liquid crystal sunset yellow. *Phys. Rev. E* **2014**, *90*, 042505.
(16) Zhou, S.; Neupane, K.; Nastishin, Y. A.; Baldwin, A. R.; Shiyanovskii, S. V.; Lavrentovich, O. D.; Sprunt, S. Elasticity, viscosity, and orientational fluctuations of a lyotropic chromonic nematic liquid crystal disodium cromoglycate. *Soft Matter* **2014**, *10*, 6571−6581.
(17) Frank, F. C. Liquid crystals. On the theory of liquid crystals. *Discuss. Faraday Soc.* **1958**, *25*, 19−28.
(18) Singh, S. Curvature elasticity in liquid crystals. *Phys. Rep.* **1996**, *277*, 283−384.
(19) Ferrarini, A. The theory of elastic constants. *Liq. Cryst.* **2010**, *37*, 811−823.
(20) Cestari, M.; Frezza, E.; Ferrarini, A.; Luckhurst, G. R. Crucial role of molecular curvature for the bend elastic and flexoelectric properties of liquid crystals: mesogenic dimers as a case study. *J. Mater. Chem.* **2011**, *21*, 12303−12308.
(21) Kaur, S.; Liu, H.; Addis, J.; Greco, C.; Ferrarini, A.; Goërtz, V.; Goodby, J. W.; Gleeson, H. F. The influence of structure on the elastic, optical and dielectric properties of nematic phases formed from bent-core molecules. *J. Mater. Chem. C* **2013**, *1*, 6667−6676.
(22) Zheng-Min, S.; Kleman, M. Measurement of the Three Elastic Constants and the Shear Viscosity γ_1 in a Main-Chain Nematic Polymer. *Mol. Cryst. Liq. Cryst.* **1984**, *111*, 321−328.
(23) Frezzato, D.; Moro, G. J.; Tittelbach, M.; Kothe, G. Transverse nuclear spin relaxation induced by director fluctuations in a nematic liquid crystal polymer. Evaluation of the anisotropic elastic constants. *J. Chem. Phys.* **2003**, *119*, 4060−4069.
(24) Hurd, A. J.; Fraden, S.; Lonberg, F.; Meyer, R. B. Field-induced transient periodic structures in nematic liquid crystals: the splay Frederiks transition. *J. Phys. (Paris)* **1985**, *46*, 905−917.
(25) Meyer, R. B.; Lonberg, F.; Taratuta, V.; Fraden, S.; Lee, S.-D.; Hurd, A. J. Measurements of the Anisotropic Viscous and Elastic Properties of Lyotropic Polymer Nematics. *Faraday Discuss. Chem. Soc.* **1985**, *79*, 125−132.
(26) Lee, S. D.; Meyer, R. B. Crossover behavior of the elastic coefficients and viscosities of a polymer nematic liquid crystal. *Phys. Rev. Lett.* **1988**, *61*, 2217−2220.
(27) Fernandes, J. R.; DuPré, D. B. In *Liquid Crystals and Ordered Fluids. 4. Proceedings of the American Chemical Society Symposium*; Griffin, A. C., Johnson, J. F., Eds.; Plenum: New York, 1984; pp 393−399.
(28) Odijk, T. Theory of Lyotropic Polymer Liquid Crystals. *Macromolecules* **1986**, *19*, 2313−2329.
(29) Meyer, R. B. In *Polymer Liquid Crystals*; Ciferri, A., Kringbaum, W. R., Meyer, R. B., Eds.; Academic Press: New York, 1982; pp 133−163.
(30) Taratuta, V. G.; Lonberg, F.; Meyer, R. B. Anisotropic mechanical properties of a polymer nematic liquid crystal. *Phys. Rev. A: At., Mol., Opt. Phys.* **1988**, *37*, 1831−1834.
(31) Odijk, T. Elastic constants of nematic solutions of rod-like and semi-flexible polymers. *Liq. Cryst.* **1986**, *1*, 553−559.
(32) Chami, F.; Wilson, M. R. Molecular Order in a Chromonic Liquid Crystal: A Molecular Simulation Study of the Anionic Azo Dye Sunset Yellow. *J. Am. Chem. Soc.* **2010**, *132*, 7794−7802.
(33) Rivas, O. M. M.; Rey, A. D. Molecular dynamics on the self-assembly of mesogenic graphene precursors. *Carbon* **2016**, *110*, 189−199.
(34) van der Schoot, P.; Cates, M. The Isotropic-to-Nematic Transition in Semi-Flexible Micellar Solutions. *Europhys. Lett.* **1994**, *25*, 515−520.
(35) Taylor, M. P.; Herzfeld, J. Shape Anisotropy and Ordered Phases in Reversibly Assembling Lyotropic Systems. *Phys. Rev. A: At., Mol., Opt. Phys.* **1991**, *43*, 1892−1905.
(36) Lü, X.; Kindt, J. T. Monte Carlo simulation of the self-assembly and phase behavior of semiflexible equilibrium polymers. *J. Chem. Phys.* **2004**, *120*, 10328−10338.
(37) Kuriabova, T.; Betterton, M. D.; Glaser, M. A. Linear aggregation and liquid-crystalline order: comparison of Monte Carlo simulation and analytic theory. *J. Mater. Chem.* **2010**, *20*, 10366−10383.
(38) De Michele, C.; Bellini, T.; Sciortino, F. Self-Assembly of Bifunctional Patchy Particles with Anisotropic Shape into Polymers Chains: Theory, Simulations, and Experiments. *Macromolecules* **2012**, *45*, 1090−1106.
(39) Sidky, H.; Whitmer, J. K. The Emergent Nematic Phase in Ionic Chromonic Liquid Crystals. *J. Phys. Chem. B* **2017**, *121*, 6691−6698.
(40) De Michele, C.; Rovigatti, L.; Bellini, T.; Sciortino, F. Self-assembly of short DNA duplexes: from a coarse-grained model to experiments through a theoretical link. *Soft Matter* **2012**, *8*, 8388−8398.
(41) Nguyen, K. T.; Sciortino, F.; De Michele, C. Self-Assembly-Driven Nematization. *Langmuir* **2014**, *30*, 4814−4819.
(42) Horowitz, V. R.; Janowitz, L. A.; Modic, A. L.; Heiney, P. A.; Collings, P. J. Aggregation behavior and chromonic liquid crystal properties of an anionic monoazo dye. *Phys. Rev. E* **2005**, *72*, 041710.
(43) Nastishin, Y. A.; Liu, H.; Schneider, T.; Nazarenko, V.; Vasyuta, R.; Shiyanovskii, S. V.; Lavrentovich, O. D. Optical characterization of the nematic lyotropic chromonic liquid crystals: Light absorption, birefringence, and scalar order parameter. *Phys. Rev. E* **2005**, *72*, 041711.
(44) Edwards, D. J.; Jones, J. W.; Lozman, O.; Ormerod, A. P.; Sintyureva, M.; Tiddy, G. J. T. Chromonic liquid crystal formation by Edicol Sunset Yellow. *J. Phys. Chem. B* **2008**, *112*, 14628−14636.
(45) Luoma, R. J. X-ray Scattering and Magnetic Birefringence Studies of Aqueous Solutions of Chromonic Molecular Aggregates (dissertation), Brandeis University, Waltham, MA, 1995.
(46) De Michele, C.; Zanchetta, G.; Bellini, T.; Frezza, E.; Ferrarini, A. Hierarchical Propagation of Chirality through Reversible Polymerization: The Cholesteric Phase of DNA Oligomers. *ACS Macro Lett.* **2016**, *5*, 208−212.

DOI: 10.1021/acs.macromol.8b00900
Macromolecules 2018, 51, 5409−5419

(47) Vieillard-Baron, J. The equation of state of a system of hard spherocylinders. *Mol. Phys.* **1974**, *28*, 809−818.
(48) O'Brien, P. A.; Allen, M. P.; Cheung, D. L.; Dennison, M.; Masters, A. Elastic constants of hard thin platelets by Monte Carlo simulation and virial expansion. *Phys. Rev. E* **2008**, *78*, 051705.
(49) Allen, M.; Frenkel, D.; Talbot, J. Molecular dynamics simulation using hard particles. *Comput. Phys. Rep.* **1989**, *9*, 301−353.
(50) Allen, M. P.; Warren, M. A.; Wilson, M. R.; Sauron, A.; Smith, W. Molecular dynamics calculation of elastic constants in Gay-Berne nematic liquid crystals. *J. Chem. Phys.* **1996**, *105*, 2850−2858.
(51) Tjipto-Margo, B.; Evans, G. T.; Allen, M. P.; Frenkel, D. Elastic constants of hard and soft nematic liquid crystals. *J. Phys. Chem.* **1992**, *96*, 3942−3948.
(52) Onsager, L. The effects of shape on the interaction of colloidal particles. *Ann. N. Y. Acad. Sci.* **1949**, *51*, 627−659.
(53) Odijk, T. Theory of lyotropic polymer liquid crystals. *Macromolecules* **1986**, *19*, 2313−2329.
(54) Parsons, J. D. Nematic ordering in a system of rods. *Phys. Rev. A: At., Mol., Opt. Phys.* **1979**, *19*, 1225−1230.
(55) Lee, S. A numerical investigation of nematic ordering based on a simple hard-rod model. *J. Chem. Phys.* **1987**, *87*, 4972−4974.
(56) McQuarrie, D. A. *Statistical Mechanics*; University Science Books: Sausalito, CA, 2000.
(57) Straley, J. P. Frank Elastic Constants of the Hard-Rod Liquid Crystal. *Phys. Rev. A: At., Mol., Opt. Phys.* **1973**, *8*, 2181−2183.
(58) Kamien, R. D.; Le Doussal, P.; Nelson, D. R. Theory of directed polymers. *Phys. Rev. A: At., Mol., Opt. Phys.* **1992**, *45*, 8727−8750.
(59) Park, H.-S.; Kang, S.-W.; Tortora, L.; Nastishin, Y.; Finotello, D.; Kumar, S.; Lavrentovich, O. D. Self-Assembly of Lyotropic Chromonic Liquid Crystal Sunset Yellow and Effects of Ionic Additives. *J. Phys. Chem. B* **2008**, *112*, 16307−16319.
(60) Renshaw, M. P.; Day, I. J. NMR Characterization of the Aggregation State of the Azo Dye Sunset Yellow in the Isotropic Phase. *J. Phys. Chem. B* **2010**, *114*, 10032−10038.
(61) Joshi, L.; Kang, S.-W.; Agra-Kooijman, D. M.; Kumar, S. Concentration, temperature, and pH dependence of sunset-yellow aggregates in aqueous solutions: an x-ray investigation. *Phys. Rev. E* **2009**, *80*, 041703.
(62) Yao, X.; Nayani, K.; Park, J. O.; Srinivasarao, M. Orientational Order of a Lyotropic Chromonic Liquid Crystal Measured by Polarized Raman Spectroscopy. *J. Phys. Chem. B* **2016**, *120*, 4508−4512.
(63) Nayani, K.; Fu, J.; Chang, R.; Park, J. O.; Srinivasarao, M. Using chiral tactoids as optical probes to study the aggregation behavior of chromonics. *Proc. Natl. Acad. Sci. U. S. A.* **2017**, *114*, 3826−3831.
(64) Chandler, D. Interfaces and the driving force of hydrophobic assembly. *Nature* **2005**, *437*, 640−647.
(65) Gemunden, P.; Daoulas, K. C. Fluctuation spectra in polymer nematics and Frank elastic constants: a coarse-grained modelling study. *Soft Matter* **2015**, *11*, 532−544.
(66) Volovik, G.; Lavrentovich, O. D. Topological dynamics of defects: boojums in nematic drops. *Sov. Phys. JETP* **1983**, *58*, 1159−1167.
(67) Lavrentovich, O. D.; Sergan, V. V. Parity-breaking phase transition in tangentially anchored nematic drops. *Nuovo Cimento Soc. Ital. Fis., D* **1990**, *12*, 1219−1222.
(68) Williams, R. D. Two transitions in tangentially anchored nematic droplets. *J. Phys. A: Math. Gen.* **1986**, *19*, 3211−3222.

DOI: 10.1021/acs.macromol.8b00900
Macromolecules 2018, 51, 5409−5419